Does Skeletal Anatomy Reflect Adaptation to Locomotor Patterns? Cortical and Trabecular Architecture in Human and Nonhuman Anthropoids

Colin N. Shaw[1,2]* and Timothy M. Ryan[1,2]

[1]*Department of Anthropology, The Pennsylvania State University, University Park, PA*
[2]*Center for Quantitative X-Ray Imaging, EMS Energy Institute, The Pennsylvania State University, University Park, PA*

KEY WORDS cortical bone; trabecular bone; anthropoids; locomotion; high-resolution computed tomography

ABSTRACT Although the correspondence between habitual activity and diaphyseal cortical bone morphology has been demonstrated for the fore- and hind-limb long bones of primates, the relationship between trabecular bone architecture and locomotor behavior is less certain. If sub-articular trabecular and diaphyseal cortical bone morphology reflects locomotor patterns, this correspondence would be a valuable tool with which to interpret morphological variation in the skeletal and fossil record. To assess this relationship, high-resolution computed tomography images from both the humeral and femoral head and mid-shaft of 112 individuals from eight anthropoid genera (*Alouatta*, *Homo*, *Macaca*, *Pan*, *Papio*, *Pongo*, *Trachypithecus*, and *Symphalangus*) were analyzed. Within-bone (sub-articular trabeculae vs. mid-diaphysis), between-bone (forelimb vs. hind limb), and among-taxa relative distributions (femoral:humeral) were compared. Three conclusions are evident: (1) Correlations exists between humeral head sub-articular trabecular bone architecture and mid-humerus diaphyseal bone properties; this was not the case in the femur. (2) In contrast to comparisons of inter-limb diaphyseal bone robusticity, among all species femoral head trabecular bone architecture is significantly more substantial (i.e., higher values for mechanically relevant trabecular bone architectural features) than humeral head trabecular bone architecture. (3) Interspecific comparisons of femoral morphology relative to humeral morphology reveal an osteological "locomotor signal" indicative of differential use of the forelimb and hind limb within mid-diaphysis cortical bone geometry, but not within sub-articular trabecular bone architecture. Am J Phys Anthropol 147:187–200, 2012.

Experimental studies have demonstrated that both diaphyseal cortical bone and sub-articular trabecular bone can respond physiologically to in vivo mechanical loading (cf. Pontzer et al., 2006; Carlson and Judex, 2007). It has also been suggested that these tissues may contain an osteological signal reflective of adaptation to locomotor behavior (Ruff and Runestad, 1992; Rafferty and Ruff, 1994). Because mechanical loadings of long bone diaphyses and articulations are certain to be quite different, one would not expect structural responses to locomotor behaviors to be necessarily similar in the two skeletal regions. Nevertheless, within the same limb a degree of correlation between the two bone structures might be expected. One might hypothesize that groups with more diverse locomotor and postural repertoires would present distinct morphological patterns. Although previous research generally supports this hypothesis for measures of diaphyseal cortical bone (e.g., Schaffler et al., 1985; Stock and Pfeiffer, 2001; Ruff, 2002; Holt, 2003; Marchi, 2008), research on the functional significance of trabecular architecture has produced a range of findings that, at present, preclude a general consensus (e.g., Fajardo and Müller, 2001; MacLatchy and Müller, 2002; Ryan and van Rietbergen, 2005; Fajardo et al., 2007; Carlson et al., 2008a; Scherf, 2008; Cotter et al., 2009; Griffin et al., 2010; Ryan and Walker, 2010; Ryan et al., 2010). If a strong locomotor signal was consistently found in both trabecular and cortical bone structure, and the signals corroborate one another, such correspondence would be a valuable tool with which to interpret variation in the skeletal and fossil record.

CORTICAL BONE MORPHOLOGY AND HABITUAL ACTIVITY PATTERNS

Experimental evidence (cf. Currey, 1984; Rubin and Lanyon, 1984, 1985; Martin et al., 1998) has revealed that long bone diaphyses respond to increased forces by structurally augmenting and redistributing their mass in the principle planes of deformation (Rubin et al., 1990; Lanyon, 1992). Although it is acknowledged that this relationship is not necessarily straightforward (Pearson and Lieberman, 2004; Ruff et al., 2006), in vivo studies have demonstrated the correspondence between habitual activity patterns and diaphyseal morphology in the human upper (cf. Jones et al., 1977; MacDougall et al., 1992; Haapasalo et al., 2000; Heinonen et al., 2002; Nikander et al., 2006) and lower limb (cf. MacDougall

Grant sponsor: National Science Foundation; Grant number: BCS-0617097.

*Correspondence to: Colin Shaw, Department of Anthropology and The Center for Quantitative X-Ray Imaging, Pennsylvania State University, University Park, PA 16802, USA. E-mail: cns12@psu.edu

Received 7 October 2010; accepted 3 October 2011

DOI 10.1002/ajpa.21635
Published online 25 November 2011 in Wiley Online Library (wileyonlinelibrary.com).

et al., 1992; Macdonald et al., 2005; Vainionpaa et al., 2007; Macdonald et al., 2009). Recent work has also described the correspondence between variation in diaphyseal torsional and average bending rigidity and shape and the habitual performance of competitive sporting activities, during adolescence (Shaw and Stock, 2009a,b). Beyond this, the relationship between habitual behavior and diaphyseal morphology is the basis upon which inferences of prehistoric hominin locomotor and manipulative activity patterns are often based (cf. Stock and Pfeiffer, 2001; Holt, 2003; Stock, 2006; Marchi, 2008; Ruff, 2008, 2009).

The influence of locomotor patterns on fore- and hindlimb diaphyseal properties has also been established in nonhuman anthropoid primate taxa. Morphological correlates for specific locomotor patterns have been described for, among others, the tibia and fibula of *Pan*, *Gorilla*, *Pongo*, and *Hylobates* (Marchi, 2007), the femora and humeri of *Pan* (Carlson, 2005; Sarringhaus et al., 2005; Carlson et al., 2008b), *Macaca*, *Trachypithecus*, and *Hylobates* (Schaffler et al., 1985) and *Papio* (Ruff, 2002), and the metatarsals and metacarpals of *Pan*, *Gorilla*, and *Pongo* (Marchi, 2005). In a broader multispecies analysis that included a diverse sample of Old World monkeys and apes, Ruff (2002) also found a general pattern where taxa associated with more forelimb suspensory locomotion displayed relatively more robust forelimbs, whereas those species whose locomotor patterns involved a greater proportion of leaping displayed relatively more robust hind limbs.

TRABECULAR BONE MORPHOLOGY AND HABITUAL ACTIVITY PATTERNS

The mechanical importance of trabecular bone structural variation has been clearly established through both experimental and modeling analyses (Radin et al., 1982; Goldstein et al., 1993; Odgaard, 1997; Kabel et al., 1999; Ulrich et al., 1999). By the end of the 20th century, evidence began to mount for the positive relationship between trabecular morphology and habitual loading (Ward and Sussman, 1979; Oxnard and Yang, 1981; Radin et al., 1982; Rafferty and Ruff, 1994; Biewener et al., 1996). With the increased availability of high-resolution computed tomography (HRCT) imaging, the testing of this relationship became more straightforward, and, as a result, within the past decade studies assessing this relationship within a range of skeletal elements and taxonomic groups have become prevalent.

One of the earlier attempts to quantitatively assess the correspondence between trabecular bone morphology and inferred locomotor patterns in multiple postcranial elements was undertaken by Rafferty and Ruff (1994) who compared humeral and femoral head trabecular mass in *Papio*, *Colobus*, and *Hylobates*. They concluded that differences in trabecular bone mass and density among these taxa corresponded to variation in the magnitude of mechanical load borne by a particular joint during locomotion. Following this, Rafferty (1998) assessed variation in trabecular and cortical bone morphology in the femoral neck of 21 nonhuman primate species and described differences in the distribution of both bone types that corresponded with hypothesized loading conditions associated with locomotion.

In partial contrast, Fajardo and Müller (2001) used HRCT to compare humeral and femoral head trabecular morphology among *Hylobates*, *Ateles*, *Macaca*, and *Papio* and found that while density-related features did not reliably differentiate suspensory climbing species from quadrupedal species, the degree of trabecular anisotropy (orientation) was more effective at doing so. Following from this, Fajardo et al. (2007) reported subtle variation in femoral neck trabecular bone distribution particular to locomotor mode, and yet overlap among all taxa (*Ateles*, *Symphalangus*, *Alouatta*, *Colobus*, *Macaca*, and *Papio*) despite differences in locomotor mode, body size, and phylogeny. Further complicating the issue is a more recent comparison of the femoral head and femoral neck trabecular morphology of *Alouatta*, *Semnopithecus*, *Papio*, *Hylobates*, and *Homo* (Scherf, 2008). Building on the work of Rafferty (1998), Scherf (2008) found more homogeneous trabecular architecture in species where relatively lower magnitude hind limb loading was performed (e.g., climbing), whereas more heterogeneous architecture was associated with specialized types of locomotion (e.g., bipedal and quadrupedal), during which, it was assumed, the hind limbs were subjected to relatively higher magnitude loading. A recent comparison of femoral and humeral head trabecular microstructure from five species of anthropoids (*Symphalangus, Papio, Trachypithecus, Alouatta,* and *Pan*), revealed broad similarities in trabecular bone structure in these bones regardless of locomotor behavior and hypothesized limb loading (Ryan and Walker, 2010). Recent experimental work that has tightly controlled the locomotor patterns of mice has also called into question the responsiveness of trabecular architecture under different loading conditions (Carlson et al., 2008a). However, the lack of response at the distal femoral metaphysis in these mice may have been influenced by the limited range of motion at the knee (e.g., predominantly flexion/extension), compared with a more proximal joint in the hind limb, such as the hip (Carlson et al., 2008a, p 391).

These results from the forelimb and hind limb of anthropoids contrast sharply with those from smaller-bodied strepsirrhine primates. Ryan and Ketcham (2002, 2005) and MacLatchy and Müller (2002) both found significant differences in trabecular bone structure of the proximal femur reflective of variation in locomotor behavior. Specifically, the trabecular architecture within the femoral heads of leaping primates (*Galago*, *Tarsius*, and *Avahi*) was found to be more anisotropic than those of nonleaping quadrupedal climbers (*Cheirogaleus*, *Loris*, and *Perodicticus*). These results indicate a strong functional signal in the femoral head trabecular bone of strepsirrhines and suggest that trabecular bone may be reflective of locomotor behavior in groups with very divergent activity patterns and loading conditions.

FOCUS OF THIS STUDY

This study includes species from eight genera within Anthropoidea, each of which can be coarsely partitioned into individual locomotor categories. The analysis of both sub-articular trabeculae and diaphyseal cortical bone is a relatively new approach (see Carlson and Judex, 2007; Carlson et al., 2008a; Lazenby et al., 2008) that allows for direct comparisons of morphological variation in two types of osseous tissue, within the same skeletal element. The integrated consideration of diaphyseal and trabecular bone properties is a perspective that attempts to move away from the reductionism that often occurs with trabecular bone analyses in the comparative literature.

The primary aim of this study is to ascertain whether variation in both sub-articular humeral and femoral head trabecular morphology, as well as humeral and femoral mid-diaphyseal structure, correspond with inferred locomotor patterns among human and nonhuman primate taxa. To assess this issue, three specific questions are asked: (1) Do diaphyseal cortical bone cross-sectional properties and sub-articular trabecular bone architectural properties within a limb co-vary, and if so, is this relationship consistent in both the humerus and the femur? (2) Do trabecular bone architecture and cortical bone morphology both contain a functional signal in the humerus and femur of anthropoids? (3) Does the distribution of cortical and trabecular bone structure between the humerus and femur reflect inferred limb usage resulting from divergent locomotor patterns among various anthropoid taxa?

MATERIALS AND METHODS

Sample

The skeletal sample used in this study consisted of one femur and one humerus from a total of 112 individuals from eight anthropoid genera (Table 1). All nonhuman specimens were wild-shot adults and exhibited no external signs of pathology or trauma. Age at death was estimated only for *Homo*. Individuals who displayed external signs of osteological senescence (i.e., osteoarthritis and eburnation) were excluded from the study. Bones from both right and left sides were used in the sample, one femur and humerus per specimen, but only elements from the same side were used for a single individual.

Trabecular bone structural analysis

All bones were scanned on the OMNI-X HD-600 high-resolution X-ray CT scanner (Varian Medical Systems, Lincolnshire, IL) at the Center for Quantitative X-Ray Imaging (CQI), The Pennsylvania State University. Each specimen was mounted in foam and positioned vertically in the scanner to collect transverse slices through the long bones. Serial cross-sectional scans were collected beginning in the shaft and proceeding proximally to cover the entire femoral or humeral head. For the femur, scans were collected beginning at or near the level of the lesser trochanter. In the humerus, scans were collected beginning just below the surgical neck and progressing proximally. All HRCT scans were collected using source energy settings of either 180 kV/0.11 mA or 150 kV/0.2 mA, between 2,800 and 4,800 views, and a Feldkamp reconstruction algorithm. The differences in energy settings resulted from a refinement of bone scanning protocols at the Penn State CQI over the last 6 years and are unlikely to affect the evaluation of trabecular structure in this study. For each scan, between 41 and 100 slices were collected during each rotation. Voxel sizes ranged between 0.027 and 0.0687 mm depending on the size of the femoral or humeral head. In all cases, the highest resolution images were obtained given the size of the specimen. The images were reconstructed as 16-bit TIFF grayscale images with a 1024 × 1024 pixel matrix.

Trabecular bone morphometric analyses were carried out on a single cubic volume of interest (VOI) extracted from the center of the femoral and humeral heads for each individual. The method for determining the size and position of the VOIs using Avizo 6.1 (Visualization

TABLE 1. Sample attributes

Genus	Species	Museum	Locomotor category	Demographics	Femoral length (mm)	Humeral length (mm)	Body mass (kg)
Alouatta	*caraya*	AMNH	Arboreal quadruped, climber	M: 3, F: 9	155.27 (8.44)	149.73 (9.35)	5.79 (0.96)[a]
Homo	*sapiens*	PSU	Biped	M: 10, F: 10	420.75 (24.40)	304.65 (17.48)	60.86 (6.41)[b]
Macaca	*fascicularis*	MCZ	Arboreal quadruped	M: 10, F: 9	131.26 (12.23)	119.55 (9.20)	4.07 (0.92)[c]
Pan	*troglodytes, verus, schweinfurthii*	AMNH	Terrestrial quadruped, climber	M: 11, F: 4, I: 2	299.55 (14.18)	305.49 (13.99)	50.13 (10.22)[d]
Papio	*anubis, cynocephalus, hamadryas, ursinus*	AMNH, NMNH	Terrestrial quadruped	M: 2, F: 4, I: 5	243.15 (33.28)	213.23 (26.01)	18.25 (4.72)[c]
Pongo	*pygmaeus, abelii*	NMNH	Quadrumanous, climber	M: 5, F: 2	280.43 (22.23)	360.86 (32.15)	65.70 (21.50)[e]
Trachypithecus	*cristatusultima*	MCZ	Arboreal quadruped	M: 9, F: 8, I: 1	173.55 (7.89)	141.28 (9.62)	5.92 (0.80)[f]
Symphalangus	*syndactylus*	NMNH	Brachiator	M: 3, F: 4	206.36 (8.52)	264.86 (11.80)	10.77 (2.48)[e]

Length and body mass data presented as: mean (standard deviation).
NMNH: National Museum of Natural History (Smithsonian Museum), Washington, USA; American Museum of Natural History, NY, USA; PSU: Norris Farms Collection, Pennsylvania State University, Department of Anthropology, MCZ: Museum of Comparative Zoology, Harvard University.
Abbreviations: M: Male, F: Female, I: Indeterminate.
Locomotor categories derived from Napier and Napier, 1967 (*Papio*); Bernstein, 1968 (*Trachypithecus*); Rodman, 1977 (*Pongo*); Curtin and and Chivers, 1978 (*Symphalangus*); Fleagle, 1988 (*Homo*); Neville et al., 1988 (*Alouatta*); Rowe, 1999 (*Macaca*); Doran, 1993 (*Pan*).
[a] Payseur et al. (1999) Haplorhine: (3.024*LN(FemHeadSI)-6.718))*1.008.
[b] Ruff et al. (1991) Male: (2.426*FemHeadAP-35.1)*0.9; Female: (2.741*FemHeadAP-54.9)*0.9.
[c] Ruff (2003) Cercopithecine: (2.389*LN(FemHeadSI)-4.541))*1.014.
[d] Ruff (2003) All hominoids: (3.019*LN(FemHeadSI)-6.668))*1.006.
[e] Ruff (2003) Asian ape: (3.024*LN(FemHeadSI)-6.718))*1.008.
[f] Ruff (2003) Colobines: (2.424*LN(FemHeadSI)-4.684))*1.01.

TABLE 2. Trabecular and cortical bone variables selected for analysis

Variable	Symbol (Unit)	Definition
Cortical bone properties		
Cortical area	CA (mm^2)	Compressive, tensile strength.
Polar second moment of area	J (mm^4)	Torsional and (twice) average bending rigidity.
Trabecular bone properties		
Bone volume fraction	BV/TV	The proportion of trabecular bone voxels to the total number of voxels in the VOI.
Connectivity density	Conn.D	The number of interconnections among trabeculae per unit volume.
Structure model index	SMI	SMI is a dimensionless measure of the relative proportion of plate-like versus rod-like structures in the VOI. Values typically range from 3 (idealized plates) to 0 (idealized rods) and can be positive or negative. Negative values indicate a more concave or closed (honey-combed) structure.
Trabecular number	Tb.N (mm^{-1})	The number of trabecular struts per mm. Calculated as the inverse distance between the mid-axes of the trabeculae.
Trabecular thickness	Tb.Th (mm)	The mean thickness of trabecular struts. Calculated using the model-independent distance transform method.
Trabecular separation	Tb.Sp (mm)	The mean distance between adjacent trabeculae. Calculated using the model-independent distance transform method.
Bone surface density	BS/BV	The ratio of trabecular bone surface area to total trabecular bone volume in the VOI. Calculated from triangulated surface reconstruction of segmented bone structure.
Degree of anisotropy	DA	DA describes the distribution of trabecular bone in three-dimensional space. The mean intercept length (MIL) method was used to calculate DA by fitting an ellipsoid to the measured MIL data. DA represents the ratio of the primary and tertiary axes of this ellipsoid. A fully isotropic structure has a DA of 1; higher values represent relatively more anisotropic structures.

Sciences Group, Burlington, MA) is detailed in Ryan and Walker (2010) and described briefly here. The articular surface of the femoral or humeral head was isolated for each specimen by manually selecting the surface triangles from a three-dimensional isosurface reconstruction. Because a precise division between articular and nonarticular regions is not possible to obtain from HRCT data alone (i.e., without other visual and physical clues present on the bones), a conservative approach was taken for all specimens to ensure that nonarticular bone was not included in the articular surface selection. The bounding box of the triangulated articular surface shell was defined as the maximum and minimum extents of the articular surface in each of the three orthogonal axes. The center of the bounding box, defined for the purposes of the current analysis as the center of the articular region, was determined by calculating the midpoints of the x, y, and z dimensions of the bounding box.

A cubic VOI was extracted from the femoral and humeral heads for trabecular bone microstructural analysis. The center of the VOI was placed at the calculated center of the articular surface bounding box and the edge length of the cube was equal to 1/6 the proximodistal height of the articular surface. This VOI selection protocol ensured that each VOI was positioned homologously (at the center of the joint) and was scaled to the size of the individual joint being analyzed. All measured variables were calculated on a sphere centered within the cubic VOI to avoid corner effects (Ketcham and Ryan, 2004). The VOIs ranged in size from $\sim$ 2.5 to 14 mm in diameter for the humerus and 2.3 to 15 mm in diameter for the femur. When analyzing trabecular structure using small VOIs, it is possible that the continuum assumption may not be satisfied (Harrigan et al., 1988). The smallest VOIs used in this study generally include a minimum of three to five intertrabecular lengths, and therefore satisfy this assumption.

The trabecular bone morphometric parameters quantified included the bone volume fraction (BV/TV), bone surface density (BS/BV), trabecular number (Tb.N), trabecular thickness (Tb.Th), trabecular separation (Tb.Sp), connectivity density (Conn.D), structure model index (SMI), and the degree of anisotropy (DA) (see Table 2 for definitions). All calculations were performed using the Scanco Image Processing Language (Scanco Medical AG, Brüttisellen, Switzerland). The HRCT images were segmented using a threshold value calculated from the iterative segmentation algorithm of Ridler and Calvard (1978; Trussell, 1979), based on the grayscale values of the VOI only. This localized segmentation approach ensured appropriate definition of the trabecular bone in the VOI. Segmented data were inspected to ensure appropriate thresholding, and the same threshold value was used for all subsequent morphometric analyses for each individual VOI. Tb.Th, Tb.Sp, and Tb.N were calculated using model-independent distance transform methods (Hildebrand and Ruegsegger, 1997a). The SMI was calculated following Hildebrand and Ruegsegger (1997b), and Conn.D was calculated following the topological approach of Odgaard and Gunderson (1993). DA was calculated using the mean intercept length method (Whitehouse, 1974; Harrigan and Mann, 1984; Cowin, 1986).

Midshaft cross-sectional geometry

The cross-sectional geometric properties of each bone were quantified from CT scans at the midshaft. The midshaft scans for most of the individuals in the sample were collected on the Penn State HRCT scanner with the same source energy settings as used for the scans of the

proximal aspect of each bone. Pixel sizes for the HRCT midshaft scans ranged from 0.027 to 0.0687 mm, depending on the size of the bone specimen. These data were reconstructed as 16-bit TIFF images with a 1024 × 1024 pixel matrix. The midshaft scans for nine of the *Pan troglodytes* specimens were collected on a Universal Systems HD-350 medical CT scanner (Universal Systems, Cleveland, OH) at CQI, The Pennsylvania State University, with slice thickness of 0.5 mm and pixel sizes between 0.29 and 0.47 mm. Images were reconstructed as 16-bit raw data with a 512 × 512 pixel matrix. Cross-sectional properties [polar section modulus (Z_p), index of maximum and minimum section modulus (Z_{max}/Z_{min}), and cortical area (CA)] calculated from 2D high-resolution midshaft images are highly significantly correlated with those same properties if recalculated from that same image following resampling to a lower spatial resolution [e.g., 0.058 mm voxel vs. 0.500 mm voxel, $n = 20$: humerus—Z_p: $r^2 = 0.998$ (percent standard error of the estimate (SEE) = 3.17), CA: $r^2 = 0.997$ (%SEE = 2.67), Z_{max}/Z_{min}: $r^2 = 0.978$ (%SEE = 2.53); femur—Z_p: $r^2 = 0.999$ (%SEE = 2.32), CA: $r^2 = 0.995$ (%SEE = 10.41), Z_{max}/Z_{min}: $r^2 = 0.975$ (%SEE = 4.04)] (Shaw and Ryan, unpublished data). Thus, the midshaft data used in this study for certain *P. troglodytes* specimens are comparable with midshaft data collected at higher resolutions for other species.

The cross-sectional geometric properties used in this analysis included the cortical area (CA) and the polar moment of inertia (J). The polar moment of inertia provides an estimate of the torsional and (twice) average bending rigidity of the bone and was calculated as the sum of the maximum and minimum second moments of area ($I_{max} + I_{min}$). The CT cross sections were individually segmented using the iterative routine of Ridler and Calvard (1978; Trussell, 1979), and the cross-sectional properties were calculated using a customized program written in Interactive Data Language v7.1 (ITT Visual Information Solutions, Boulder, CO).

Body mass estimation

Body mass for each individual was estimated from femoral head dimensions using equations derived from analyses of the most appropriate taxonomic group (Table 1). Femoral head antero–posterior breadth, medio–lateral breadth, and supero–inferior height were measured to the nearest hundredth millimeter using digital calipers.

Statistical analysis

Partial correlation analyses controlling for body mass were used to test the association between the raw cortical bone variables and each of the raw trabecular bone variables for the femur and humerus separately. Differences in trabecular bone architecture and cortical bone structure between the humerus and the femur were also tested within each taxon using paired-samples *t*-tests. To test for interspecific variation in femoral vs. humeral proportions, log transformed (Log10) hind limb/forelimb indices were calculated for each raw cortical and trabecular bone variable, and an ANOVA was used to test for differences among species. In cases where ANOVA demonstrated a significant difference in hind limb to forelimb ratios, Tukey's or Games-Howell post hoc test was used to identify between-species differences. For all statistical tests, null hypotheses were rejected for *P*-values less than 0.05.

TABLE 3. Partial correlation (controlling for body mass) between femoral and humeral midshaft (CA and J) and trabecular bone properties, for all species

		Humeral		Femoral	
	n	r^2	P	r^2	P
CA vs.					
BV/TV	110	0.457	0.000*	0.047	0.621
Conn.D	110	0.046	0.628	−0.124	0.195
SMI	110	−0.444	0.000*	−0.105	0.275
Tb.N	110	0.184	0.053	−0.103	0.281
Tb.Th	110	0.079	0.407	−0.015	0.874
Tb.Sp	110	−0.294	0.002*	0.094	0.325
BS/BV	110	−0.200	0.035*	−0.111	0.248
DA	109	0.030	0.755	0.147	0.125
J vs.					
BV/TV	110	0.505	0.000*	−0.006	0.947
Conn.D	110	0.162	0.089	0.061	0.522
SMI	110	−0.472	0.000*	−0.029	0.765
Tb.N	110	0.309	0.001*	0.094	0.327
Tb.Th	110	−0.030	0.756	−0.182	0.056
Tb.Sp	110	−0.431	0.000*	−0.065	0.500
BS/BV	110	−0.126	0.188	0.072	0.454
DA	109	−0.033	0.734	0.161	0.093

* Significant relationship ($P \leq 0.05$).

Although Swartz et al. (1989) found little dependence of trabecular length and width on body mass, Doube et al. (2011) recently suggested that certain trabecular architectural features (Tb.Th, Tb.N, and Tb.Sp) are, in fact, significantly influenced by body mass. This result suggests that some standardization of trabecular bone architectural features should be considered in interspecific comparisons. Possible variables for normalizing trabecular bone features include estimates of body mass and overlying articular surface area.

A method has not yet been developed to standardize measures of trabecular bone architecture for variation in body mass or articular surface area for the primate taxa included in this study. Furthermore, it has not been demonstrated that such a standardization is necessary for inter-specific comparisons within Primates. Most of the variables used in this study, and in most other studies of trabecular bone, are already standardized by volume or length (e.g., BV/TV and Conn.D) or dimensionless (SMI) and show no significant relationship with body mass or articular surface area. Others, such as Tb.Th, Tb.N, and Tb.Sp, show either no relationship with body mass or articular surface area or display a very low level of correlation and a large amount of variation, which makes standardization difficult. The extent of trabecular bone structural heterogeneity within the humeral and femoral heads is as yet unstudied; furthermore, the amount of intraspecific structural variation in the VOI used in this study is high. Thus, standardizing a discrete VOI by a measurement such as femoral or humeral head articular surface area may serve to inadvertently increase variation and make functional interpretations more difficult. Therefore, we have taken the approach of presenting unstandardized measures of trabecular architecture that can, if necessary, be reinterpreted if more appropriate methods are developed in the future.

Although it has been argued that comparisons of polar second moment of area (J) require the use of bone length as a proxy for moment arm length, this is unlikely to be accurate when comparing taxa that do not have comparable relative limb lengths (Ruff, 2000). For taxa such as siamangs and orangutans, with their greatly elongated

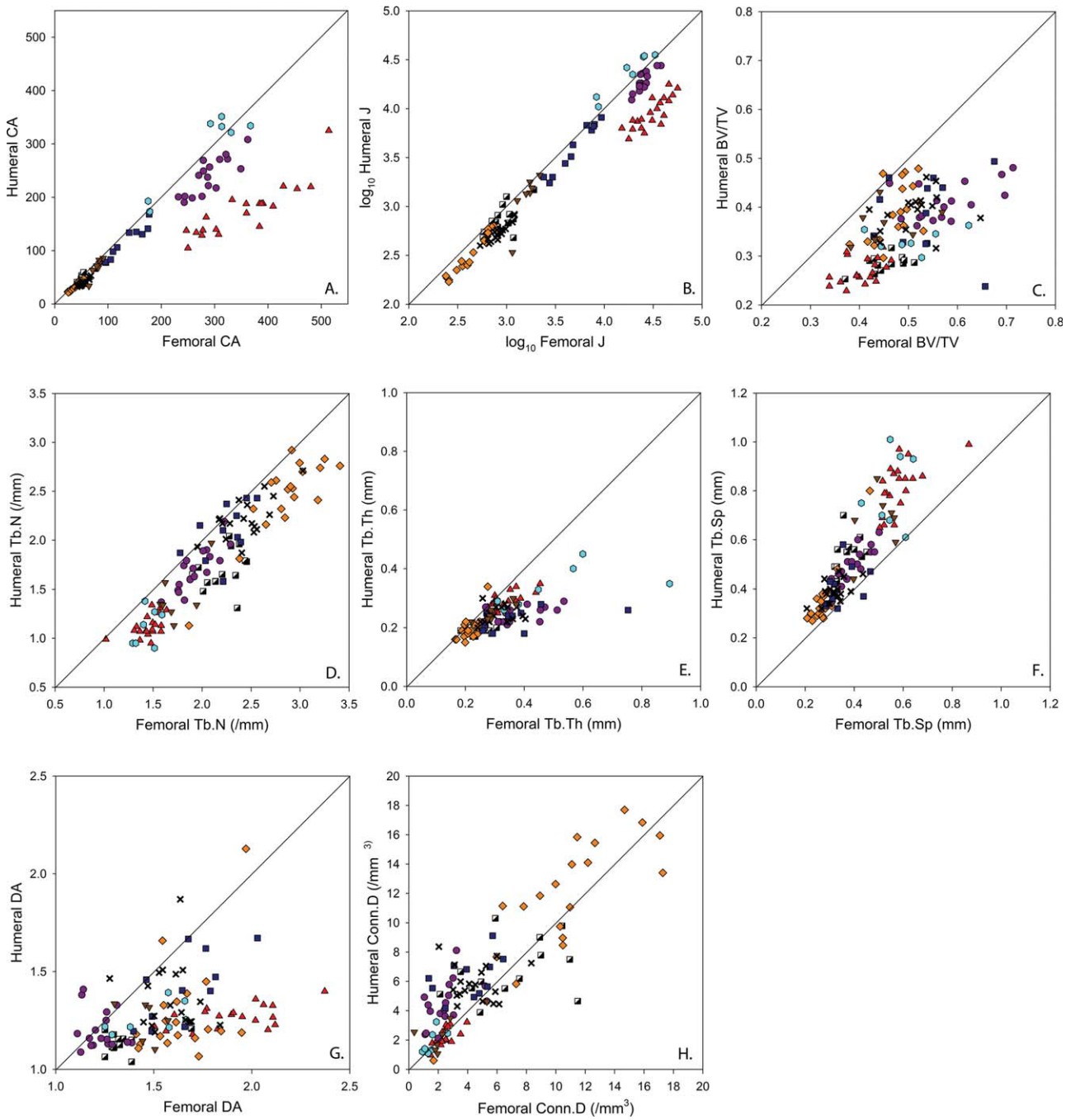

Fig. 1. Comparison of femoral and humeral bone structure for each individual in the sample. The lines in each graph represent similarity between the humeral and femoral measurements for each variable. (**A**) Midshaft cortical area (CA), (**B**) midshaft torsional rigidity (J), (**C**) bone volume fraction (BV/TV), (**D**) trabecular number (Tb.N), (**E**) trabecular thickness (Tb.Th), (**F**) trabecular separation (Tb.Sp), (**G**) degree of anisotropy (DA), and (**H**) connectivity density (Conn.D). *Alouatta* (◪), *Homo* (▲), *Macaca* (◆), *Papio* (■), *Pan* (●), *Pongo* (⬢), *Symphalangus* (▼), and *Trachypithecus* (✖).

forelimbs, limb length is not proportional to true moment arm length in the same way that it would be in a taxon such as Papio. Additionally, phylogenetic corrections were not conducted for the data considered here; significant effects are not expected for size-adjusted cortical bone structure (O'Neill and Dobson, 2008), and further investigation is required to determine whether phylogenetic variation influences primate trabecular bone architecture (Swartz, 1989; Doube et al., 2011).

RESULTS

Cortical vs. trabecular bone correlations

Partial correlations controlling for body mass were performed to compare CA and J, separately, against each trabecular bone variable from both the humerus and femur (Table 3). For the humerus, J and CA are significantly, and positively, correlated with BV/TV, while a

similar relationship is also found between humeral J and Tb.N. Additionally, the relationship between humeral CA and Tb.N approaches significance ($P = 0.053$). Humeral CA and J are also significantly, yet negatively, correlated with Tb.Sp and SMI. In contrast, comparisons for the femur reveal no significant relationships between midshaft cortical bone cross-sectional properties and trabecular architectural properties.

Femur vs. humerus: Trabecular and cortical morphology

Paired sample *t*-tests (2-tailed) were performed for each taxon to assess differences between humeral and femoral midshaft diaphyseal properties (CA and J) (Table 4). Measures of both CA and J are significantly greater in the femur compared with the humerus for seven of eight taxa, with comparisons of J for *Alouatta* and *Symphalangus* just reaching significance (Fig. 1a,b). In direct contrast, within *Pongo* measures of J are significantly greater in the humerus than the femur, whereas CA is higher in the humerus compared with the femur, but not significantly so.

Paired samples *t*-tests (2-tailed) were also performed for each taxon comparing femoral head trabecular bone variables against humeral head trabecular bone variables (Table 5). Comparisons of BV/TV, Tb.N, and Tb.Th reveal that for all species femoral head measures are significantly greater than humeral head measures (Fig. 1c–e). The single exception to this trend was found for the comparison of Tb.N within *Papio*, where significant differences are not found. The opposite is true for Tb.Sp where all species display Tb.Sp that is significantly greater in the humeral head compared to the femoral head (Fig. 1f). These results indicate that regardless of taxonomic (or locomotor) classification, femoral head Tb.Th and Tb.N are significantly greater than in the humeral head. As a result, the relative amount of trabecular bone in the femoral head (BV/TV) is greater than in the humeral head.

Across virtually all taxa, femoral head trabecular bone is significantly more anisotropic (greater DA) than trabecular bone in the humeral head, which reflects a more uniform trabecular orientation in the latter (Fig. 1g). The outlier for this comparison is *Pan*, where no significant differences are found between femoral and humeral head DA. The BS/BV, the ratio of trabecular bone surface area to trabecular volume, and SMI are significantly greater in the humeral head compared to the femoral head for all but one taxon, *Symphalangus* (for SMI, the difference only approaches significance). In contrast, comparisons of Conn.D do not reveal such an obvious pattern; significant differences are found only within *Pan*, *Papio*, and *Trachypithecus* (Fig. 1h).

Hind limb/forelimb trabecular and cortical morphology variation between taxa

Table 6 displays the mean and standard deviations for the cortical and trabecular bone variables included in the analyses, presented as ratios (femoral property:humeral property). Table 7 displays the *P*-values for the among-species ANOVA comparisons for all log-transformed (log10) cortical bone (CA and J) and trabecular bone (BV/TV, Tb.N, and Tb.Th) variable indices. These particular trabecular bone variables were included in this analysis as a result of their significant, positive rela-

TABLE 4. Paired samples t-test (2-tailed): Femoral vs. humeral midshaft properties, by species

	Alouatta	Homo	Macaca	Pan	Papio	Pongo	Trachypithecus	Symphalangus
CA								
Humerus	47.40	175.21	32.97	239.41	111.93	291.95	39.17	68.69
Femur	52.88	354.90	38.05	289.21	129.02	281.52	52.21	79.19
Diff. (SE)	−5.48 (1.90)	−179.70 (9.53)	−5.08 (0.389)	−49.79 (5.32)	−17.09 (2.86)	10.43 (10.57)	−13.04 (0.590)	−10.49 (3.60)
P	0.014*	0.000*	0.000*	0.000*	0.000*	0.362	0.000*	0.027*
J								
Humerus	797.98	9565.73	377.55	19178.65	4557.37	25284.87	559.45	1379.98
Femur	961.15	32339.24	488.34	25272.77	5484.90	19673.93	861.60	1646.04
Diff. (SE)	−163.16 (73.70)	−22773.51 (1965.58)	−110.78 (8.91)	−6094.12 (601.01)	−927.53 (145.61)	5610.93 (1266.33)	−302.15 (19.34)	−266.06 (103.92)
P	0.047*	0.000*	0.000*	0.000*	0.000*	0.004*	0.000*	0.043*

Diff.: mean paired difference (humerus-femur), SE: standard error of mean paired difference.
* $P \leq 0.05$.

TABLE 5. Paired samples t-test (2-tailed): Femoral vs. humeral sub-articular trabecular properties, by species

	Alouatta	Homo	Macaca	Pan	Papio	Pongo	Trachypithecus	Symphalangus
BV/TV								
Humerus	0.288	0.265	0.387	0.410	0.394	0.333	0.390	0.366
Femur	0.460	0.401	0.472	0.577	0.535	0.507	0.510	0.456
Diff. (SE)	−0.172 (0.009)	−0.136 (0.008)	−0.085 (0.011)	−0.166 (0.015)	−0.141 (0.033)	−0.175 (0.026)	−0.120 (0.013)	−0.089 (0.024)
P	0.000*	0.000*	0.000*	0.000*	0.002*	0.001*	0.000*	0.010*
Conn.D								
Humerus	6.76	2.17	11.70	4.44	6.29	1.87	5.88	2.44
Femur	6.95	2.32	10.66	2.52	4.06	1.57	4.53	2.35
Diff. (SE)	−0.191 (0.819)	−0.150 (0.107)	1.04 (0.559)	1.91 (0.345)	2.23 (0.495)	0.303 (0.222)	1.36 (0.458)	0.093 (0.400)
P	0.820	0.176	0.079	0.000*	0.001*	0.222	0.009*	0.822
SMI								
Humerus	0.441	0.802	−0.542	−1.23	−0.765	−0.022	−0.467	−1.16
Femur	−1.53	−0.787	1.69	−4.95	−3.02	−2.59	−2.62	−2.04
Diff. (SE)	1.97 (0.200)	1.59 (0.121)	1.14 (0.196)	3.73 (0.560)	2.26 (0.847)	2.57 (0.425)	2.15 (0.450)	0.875 (0.386)
P	0.000*	0.000*	0.000*	0.000*	0.024*	0.001*	0.000*	0.064
Tb.N								
Humerus	1.70	1.12	2.44	1.70	2.09	1.12	2.23	1.42
Femur	2.22	1.45	2.85	1.94	2.24	1.44	2.44	1.75
Diff. (SE)	−0.518 (0.063)	−0.330 (0.027)	−0.411 (0.049)	−0.233 (0.028)	−0.148 (0.074)	−0.318 (0.066)	−0.215 (0.045)	−0.323 (0.082)
P	0.000*	0.000*	0.000*	0.000*	0.073	0.003*	0.000*	0.007*
Tb.Th								
Humerus	0.192	0.288	0.197	0.244	0.233	0.337	0.244	0.250
Femur	0.256	0.333	0.220	0.373	0.373	0.504	0.311	0.298
Diff. (SE)	−0.065 (0.009)	−0.045 (0.008)	−0.023 (0.007)	−0.129 (0.018)	−0.140 (0.040)	−0.167 (0.066)	−0.068 (0.012)	−0.048 (0.012)
P	0.000*	0.000*	0.007*	0.000*	0.006*	0.044*	0.000*	0.006*
Tb.Sp								
Humerus	0.533	0.819	0.357	0.495	0.406	0.803	0.386	0.671
Femur	0.369	0.585	0.278	0.394	0.346	0.553	0.318	0.499
Diff. (SE)	0.165 (0.019)	0.234 (0.018)	0.079 (0.017)	0.101 (0.009)	0.061 (0.023)	0.250 (0.058)	0.068 (0.010)	0.171 (0.046)
P	0.000*	0.000*	0.000*	0.000*	0.027*	0.005*	0.000*	0.010*
BS/BV								
Humerus	11.75	8.48	11.23	8.20	9.42	6.98	9.21	8.44
Femur	8.56	6.85	9.43	5.33	6.19	4.88	6.85	7.07
Diff. (SE)	3.19 (0.441)	1.62 (0.156)	1.81 (0.356)	2.87 (0.291)	3.22 (0.675)	2.10 (0.262)	2.36 (0.316)	1.37 (0.356)
P	0.000*	0.000*	0.000*	0.000*	0.001*	0.000*	0.000*	0.008*
DA								
Humerus	1.13	1.27	1.29	1.20	1.42	1.26	1.37	1.25
Femur	1.34	1.89	1.65	1.23	1.66	1.48	1.58	1.46
Diff. (SE)	−0.206 (−0.206)	−0.624 (0.044)	−0.357 (0.054)	−0.030 (0.034)	−0.241 (0.044)	−0.224 (0.053)	−0.216 (0.052)	−0.213 (0.065)
P	0.000*	0.000*	0.000*	0.397	0.000*	0.005*	0.001*	0.022*

Diff.: mean paired difference (humerus-femur), SE: standard error of mean paired difference.* $P \leq 0.05$.

TABLE 6. Average (raw) femur:humerus ratio values for both diaphyseal cortical and sub-articular trabecular bone variables

	J	CA	BV/TV	Tb.N	Tb.Th
Alouatta	1.27 (0.43)	1.13 (0.16)	1.60 (0.11)	1.32 (0.18)	1.34 (0.17)
Homo	3.47 (0.80)	2.06 (0.25)	1.53 (0.17)	1.30 (0.13)	1.15 (0.11)
Macaca	1.33 (0.13)	1.15 (0.05)	1.24 (0.15)	1.19 (0.14)	1.13 (0.15)
Pan	1.34 (0.15)	1.22 (0.10)	1.41 (0.15)	1.14 (0.08)	1.52 (0.29)
Papio	1.27 (0.19)	1.16 (0.08)	1.43 (0.48)	1.08 (0.14)	1.61 (0.53)
Pongo	0.77 (0.11)	0.97 (0.09)	1.53 (0.21)	1.31 (0.20)	1.48 (0.49)
Trachypithecus	1.54 (0.12)	1.34 (0.06)	1.31 (0.17)	1.10 (0.09)	1.29 (0.22)
Symphalangus	1.45 (0.88)	1.21 (0.31)	1.25 (0.17)	1.25 (0.19)	1.18 (0.11)

Data presented as: Ratio (SD).

tionship with cortical bone torsional and average bending rigidity and area (Table 3). For J and CA, *Homo* displays significantly greater ratios than all other species. Similarly, *Trachypithecus* also displays ratios for J and CA that are significantly greater than most taxa, excluding *Homo*, *Symphalangus*, and *Alouatta* (J only). In contrast, ratios of J and CA displayed by *Pongo* are significantly lower than those of all other taxa (save for *Symphalangus*). There are no significant differences for these measurements among *Pan, Papio, Symphalangus, Macaca*, and *Alouatta*.

DISCUSSION

Correlation between cortical vs. trabecular bone morphology

The primary aim of this study was to determine how well variation in sub-articular humeral and femoral head trabecular architecture, and also mid-diaphysis cross-sectional properties, correspond with variation in inferred locomotor patterns in a diverse sample of human and nonhuman primate taxa. The results of the first analysis indicate that, after controlling for body mass, diaphyseal cortical bone properties and trabecular bone properties do co-vary within the humerus, but not the femur. Generally, in the humerus, the amount of trabecular bone increases in concordance with increasing cortical diaphyseal strength (both area as well as torsional and average bending rigidity). This suggests that in spite of the very different strain regimes between the epiphyses and diaphyses, when the humerus as a whole is "loaded," the morphological response to applied loading between the two regions, although different, appears somewhat consistent. These results indicate that in the humerus an increase in trabecular bone is accomplished by adding trabeculae (increasing Tb.N) rather than by simply increasing the thickness of existing trabeculae. This process creates a more densely packed "honeycomb-like" trabecular structure (negative SMI) and increases the relative amount of bone (BV/TV) in the VOI (Table 3).

The same conclusion cannot be made for the analogous location in the femur. The lack of a significant relationship between cortical and trabecular bone properties in the femur may be multifactorial. It could be that the VOI selected for the femoral head has not captured biomechanically relevant trabecular structure. Perhaps more relevant, when loaded in vivo the joint and the diaphysis of both the femur and humerus will be subjected to different types of strain (primarily bending and torsion at the diaphysis, and compression upon the articular surface) and also different strain parameters (magnitude, frequency, and rate). Although it is reasonable to assume that the entire bone is "loaded" at various time-points throughout the gait cycle, the imposition of strain types and parameters will be particular to each location. Although one might expect a degree of correlation between the adaptation of the diaphysis and sub-articular trabeculae within the same bone, it is unreasonable to assume that osteological adaptations will be similar in each location. This variability in the quality and magnitude of strain may help to explain structural differences in various locations within a single bone. Gross structural differences between the humerus and femur (and differences in the strain patterns particular to each bone) may, in part, be responsible for the lack of co-variation found between trabecular architecture and diaphyseal geometry in the femur, and the contrasting positive covariation in the humerus. Although one could model the humerus as a single beam the femur is more reasonably modeled as a two connected beams (diaphysis and neck). Although compression at the articular ends of the humerus could create axial compressive loads superimposed upon bending loads likely to be experienced at the humeral diaphysis during movement, compression at the femoral head would not necessarily translate similarly to the femoral mid-diaphysis.

Femur vs. humerus: Differences in trabecular and cortical bone morphology

For all but one taxon included in this study, diaphyseal cortical bone area (CA) and torsional and average bending rigidity (J) was significantly greater in the femur than the humerus. In contrast, cortical bone area was higher, and torsional and average bending rigidity were significantly greater in the humerus within *Pongo*.

Overall, this variation among taxa does to some degree reflect locomotor behaviors. For an obligate biped, such as *Homo*, it is reasonable to expect that greater loading of the hind limbs (relative to the forelimbs) would result in a femoral midshaft that is more robust than the humeral midshaft. Juxtaposed with a bipedal gait, it may also be reasonable to expect that quadrumanous climbing and brachiation, as performed by *Pongo* and *Symphalangus*, respectively, would be associated with more robust upper limbs (in comparison with the lower limbs). Although femoral cortical area and torsional and average bending rigidity were significantly greater in the femur than the humerus of *Symphalangus*, within *Pongo*, the torsional and average bending rigidity of the humeral diaphysis were significantly greater than that of the femur. Brachiation, as performed by *Symphalangus*, may not impose the forces on the upper limbs that are necessary to induce diaphyseal adaptation in the same way that bipedal and quadrupedal locomotion appear to in other taxa (Swartz et al., 1989). It has been suggested

TABLE 7. P-values for post hoc (ANOVA) comparisons of log transformed (Log10) indices (femur:humerus) among species for cortical and trabecular bone variables

	Alouatta	*Homo*	*Macaca*	*Pan*	*Papio*	*Pongo*	*Trachypithecus*	*Symphalangus*
A								
J								
Alouatta	X	0.002*	0.957	0.956	1.000	0.004*	0.168	1.000
Homo		X	0.000*	0.000*	0.000*	0.000*	0.000*	0.010*
Macaca			X	1.000	0.954	0.000*	0.000*	1.000
Pan				X	0.957	0.000*	0.005*	1.000
Papio					X	0.000*	0.016*	1.000
Pongo						X	0.000*	0.147
Trachypithecus							X	0.965
Symphalangus								X
B								
CA								
Alouatta	X	0.000*	0.977	0.575	0.989	0.125	0.008*	0.995
Homo		X	0.000*	0.000*	0.000*	0.000*	0.000*	0.004*
Macaca			X	0.539	1.000	0.014*	0.000*	1.000
Pan				X	0.790	0.002	0.007*	1.000
Papio					X	0.012*	0.001*	1.000
Pongo						X	0.000*	0.346
Trachypithecus							X	0.823
Symphalangus								X
C								
BV/TV								
Alouatta	X	1.000	0.000*	0.269	0.214	1.000	0.004*	0.005*
Homo		X	1.000	0.892	0.779	1.000	0.033*	0.033*
Macaca			X	0.134	0.618	0.023*	0.993	1.000
Pan				X	1.000	0.997	0.979	0.753
Papio					X	0.980	1.000	1.000
Pongo						X	0.377	0.210
Trachypithecus							X	1.000
Symphalangus								X
D								
Tb.N								
Alouatta	X	1.000	0.225	0.022*	0.001*	1.000	0.000*	1.000
Homo		X	0.232	0.017*	0.000*	1.000	0.000*	1.000
Macaca			X	1.000	0.457	0.762	0.637	1.000
Pan				X	0.987	0.229	1.000	0.919
Papio					X	*.014	1.000	0.186
Pongo						X	0.019*	1.000
Trachypithecus							X	0.286*
Symphalangus								X
E								
Tb.Th								
Alouatta	X	0.488	0.203	0.809	0.625	1.000	1.000	0.988
Homo		X	1.000	0.000*	0.001*	0.156	0.916	1.000
Macaca			X	0.000*	0.000*	0.061	0.588	1.000
Pan				X	1.000	1.000	0.146	0.081
Papio					X	1.000	0.105	0.054
Pongo						X	0.975	0.705
Trachypithecus							X	1.000
Symphalangus								X

Raw (femur:humerus) indices used in these analyses (ANOVA) are available in Table 6.
* Significant relationship ($P \leq 0.05$).

that in other brachiating species, such as *Hylobates*, brachiation subjects the forelimbs to tensile and muscle-generated compressive forces, which are likely to be smaller than bending and torsional forces engendered during cursorial locomotion (Swartz et al., 1989; Patel and Carlson, 2008). The influence of loading on skeletal adaptation is complex and requires the quantification of numerous variables, including load magnitude and frequency (Shaw and Stock, 2009b). Fleagle (1976) reported that up to 62% of the locomotor bouts recorded by *Symphalangus* were behaviors such as climbing and bipedal walking or hopping in which the hind limb is actively used (see Ryan and Walker, 2010 for further discussion).

The differences between forelimb and hind limb diaphyseal structure in arboreally quadrupedal *Trachypithecus*, *Alouatta*, and *Macaca*, and terrestrially quadrupedal *Pan* and *Papio*, most likely reflect adaptation to primarily hind limb driven locomotor patterns, a strategy that has been documented in various primate taxa (Kimura, 1985, 1992; Demes et al., 1994; Hanna et al., 2006) (see discussion below).

In partial contrast with comparisons of diaphyseal torsional and average bending rigidity and bone area performed in this study, comparisons of trabecular bone morphology are quite consistent; femoral head sub-articular trabecular architecture is significantly more substantial than humeral head sub-articular trabecular structure (Table 5), having more and thicker trabeculae resulting in higher BV/TV. This pattern of hind- to fore-limb trabecular proportion is consistent

among virtually all taxa, regardless of differences in locomotor behavior.

The taxa included in this study were subjectively partitioned into somewhat discrete locomotor groups to test the hypothesis that cortical and trabecular morphology would (differentially) adapt to, and therefore reflect, differences in these locomotor patterns. However, it has been suggested that commonalities exist in the loading patterns of anthropoids, regardless of gait characteristics. Demes et al. (1994) compared force plate data collected on *Pan*, *Pongo*, and *Chlorocebus* (vervet monkey), throughout a range of terrestrial gaits and speeds. The goal of this research was to assess variation in peak vertical forces acting on the fore and hind limbs as well as the braking and propulsive impulses. The results indicated that although reaction forces are highly variable, and change with speed and gait, among all primates included in this study, vertical peak reaction forces are higher on the hind limbs than the forelimbs, and that in most cases the major propulsive thrust is generated by the hind limbs. However, not to be discounted, forelimb braking as performed during quadrupedal travel (Demes et al., 2006; Demes and Carlson, 2009), and landing following a leaping bout (Demes et al., 2005), also generates large ground reaction forces at the forelimbs and could also influence the associated bone structure.

Although Demes et al. (1994) present compelling evidence to explain the fore and aft asymmetry seen here for primarily terrestrial taxa, studies that have measured external forces during nonterrestrial travel are equally informative given the inclusion of a few (primarily) arboreal species in this study. Hirasaki et al. (2000) have shown that during vertical climbing both Japanese macaques and spider monkeys load their hind limbs to a greater degree than their forelimbs, even though macaques were shown to use their forelimbs to aid in propulsion. Additionally, Schmitt and Hanna (2004) analyzed seven primate species and found that peak vertical reaction forces are greater in the hind limb (relative to the forelimb) in an arboreal context compared with a terrestrial context. The general dominance of the hind limb in primate locomotion is likely to have a major influence on the morphological variation reported here. Additional research that examines the imposition of forces on primate limbs during a range of activities while assessing in vivo loading patterns during brachiation and *Pongo*-specific quadrumanous movement is clearly warranted to bring further clarity to the morphological variation described here.

Interspecific comparisons—Hind limb:forelimb ratios for trabecular and cortical bone morphology

Although the epiphyses and diaphyses experience very different strain regimes, a limb that encounters relatively large loads would be expected to display relatively higher diaphyseal robusticity and higher sub-articular trabecular mass (Ruff and Runestad, 1992; Rafferty and Ruff, 1994). *Homo* and (to a lesser extent) *Trachypithecus* both display greater relative hind limb diaphyseal robusticity (femur:humerus) compared with virtually all other taxa. *Pongo*, by contrast, displays torsional and average bending rigidity and cortical area inter-limb ratios that are significantly lower than those of all other taxa (save for *Symphalangus*, where differences are not significant). Interspecific comparisons of trabecular bone morphology do not reveal a comparable pattern. These results indicate that for the anthropoid taxa included here, the distribution of femoral to humeral diaphyseal robusticity does reflect adaptation to inferred locomotor patterns, whereas the same cannot be said for femoral and humeral head sub-articular trabecular bone architecture.

Prior comparisons involving anthropoid taxa have reported a similarly pronounced relationship between inferred locomotor behavior and the distribution of fore- and hind-limb diaphyseal robusticity (e.g., Schaffler et al., 1985; Ruff and Runestad, 1992; Ruff, 2002). Ruff (1987) found that, among great apes, orangutans displayed the weakest hind limb diaphyses, apparently because of a higher frequency of forelimb suspensory behavior and relative unloading of the hind limb. Similarly, Schaffler et al. (1985) concluded that among *Macaca, Trachypithecus*, and *Hylobates* the ratio of humeral to femoral bending rigidity could be used to identify trends toward hind limb or forelimb dominance during locomotion.

In partial contrast to the results presented here, Fajardo and Müller (2001) found that as measures of BV/TV did not reliably differentiate suspensory climbing species from quadrupedal species, variation in the DA at the femoral head-neck transition was a relatively accurate predictor. However, similar to the results presented here, previous comparisons of trabecular bone structure within the femoral and humeral head (Ryan and Walker, 2010), and femoral neck (Fajardo et al., 2007), indicate a broad similarity in the sub-articular structure of these bones across anthropoids. Fajardo and Müller (2001) (to a less obvious degree), Fajardo et al. (2007), and Ryan and Walker (2010), and the results from this study were unable to find a strong and consistent trabecular signal reflective of the locomotor behaviors of terrestrial and suspensory anthropoids. This contrasts with studies showing differences in femoral head trabecular structure between leaping and climbing taxa (Ryan and Ketcham, 2002, 2005). MacLatchy and Müller (2002) also identified a locomotor signal related to femoral head and neck trabecular anisotropy (DA) (but not relative bone volume) that differentiated *Perodicticus* from *Galago*. It may be that compared with leaping-based locomotion, bipedal, quadrupedal, or suspensory locomotor patterns do not load the limbs in a manner that elicits structural adaptation in femoral or humeral head trabecular architecture. The broad similarities in hip joint loading between bipeds and quadrupeds (Bergmann et al., 1984; Bergmann et al., 1993, 1999), taken in concert with the general similarity in trabecular bone structure across anthropoids and other mammals (Kummer, 1972; Pauwels, 1980a,b), suggests that the trabecular structure of the proximal femur may not contain a strong locomotion-specific signal (Rafferty, 1998; Fajardo et al., 2007).

CONCLUSIONS

Overall, three primary conclusions are evident: (1) It appears that within anthropoids, measures of humeral head trabecular architecture and diaphyseal structure significantly co-vary. Equivalent relationships are not apparent in the femur. (2) In contrast to comparisons of inter-limb diaphyseal bone robusticity, across all species femoral head trabecular bone architecture is significantly more substantial than that found within the

humeral head. (3) Interspecific comparisons of femoral bone structure relative to humeral bone structure indicate that while an osteological "locomotor signal" is apparent within cortical bone, the same cannot be said for trabecular bone. Previous research has demonstrated a correlation between trabecular bone-mass, quantified using 2D radiographic images, and locomotor behavior, possibly because this variable reflects the magnitude of loading across the joint (Rafferty and Ruff, 1994). In this study, individual trabecular bone architectural properties, calculated from 3D high-resolution CT data, did not vary in a systematic manner between species, and may reflect intrinsic physiological limitations associated with sub-articular osseous structure.

Although the results of this study are relatively straightforward, providing commentary on general trabecular bone adaptation may prove erroneous. The necessary caveats to the conclusions stated above are multiple: although consistency in trabecular morphology was demonstrated across all taxa in the analysis, further testing is required to assess how applicable these results are to other regions within the hip and shoulder joints, other bones in the skeleton, other anthropoid species, and other primates in general. Although species with an array of locomotor behaviors were included, the next step is to broaden the sample to include additional locomotor patterns (e.g., leapers) and taxa with a wider array of body sizes.

The hip and shoulder joints are complex structures that allow for loading in various dimensions. This variability is likely to have influenced the results of the current study. Future investigations of this type may consider assessing more constrained joints in the skeleton (Carlson et al., 2008a; Lazenby et al., 2008; Griffin et al., 2010; Ryan et al., 2010). The hind limb dominance of most anthropoids undoubtedly influences the distribution of cortical bone robusticity and trabecular bone architectural properties. The ability to control for this variability when analyzing cortical and trabecular bone structure would provide a more nuanced understanding of the influence that locomotor patterning has on skeletal and fossil morphology (Carlson and Judex, 2007; Carlson et al., 2008a). VOI, the area from which trabecular measurements are taken, can be extracted from multiple areas within a given anatomical region (e.g., the femoral head). Although VOI location was standardized in this study, further investigation is required to assess how trabecular morphology varies throughout a sub-articular region, and how variation in VOI location affects functional interpretations. Finally, a multivariate approach that accounts for a greater proportion of the inherent variation in trabecular morphology (as opposed to pairwise species comparisons using a single variable) would potentially provide a powerful approach for assessing the correspondence between the biomechanical form of trabecular bone and locomotor and other activity patterns.

ACKNOWLEDGMENTS

The authors thank Alan Walker for his support and helpful suggestions during the course of this project. They also thank Darrin Lunde and Eileen Westwig at the American Museum of Natural History, Richard Thorington and Linda Gordon at the National Museum of Natural History, Smithsonian Institution, Judith Chupasko at the Museum of Comparative Zoology, Harvard University, George Milner at Pennsylvania State University, and Terrance Martin at the Illinois State Museum for their assistance with specimens and their willingness to loan specimens for scanning. Thanks to T. Stecko, I. Carlson, M. Test, L. Souza, S. Kobos, A. Placke, A. Swiatoniowski, and K. Hunsicker who helped with various aspects of image acquisition, processing, and data entry.

LITERATURE CITED

Bergmann G, Graichen F, Rohlmann A. 1993. Hip joint loading during walking and running measured in two patients. J Biomech 26:969–990.

Bergmann G, Graichen F, Rohlmann A. 1999. Hip joint forces in sheep. J Biomech 32:769–777.

Bergmann G, Siraky J, Rohlmann A. 1984. A comparison of hip joint forces in sheep, dog, and man. J Biomech 17:907–921.

Bernstein I. 1968. The latong of Kuala Selangor. Behaviour 32:1–16.

Biewener A, Fazzalari N, Konieczynski D, Baudinette R. 1996. Adaptive changes in trabecular architecture in relation to functional srain patterns and disuse. Bone 19:1–8.

Carlson K. 2005. Investigating the form-function interface in African apes: relationships between principal moments of area and positional behaviours in femoral and humeral diaphyses. Am J Phys Anthropol 127:312–334.

Carlson K, Judex S. 2007. Increased non-linear locomotion alters diaphyseal bone shape. J Exp Biol 210:3117–3125.

Carlson K, Lublinsky S, Judex S. 2008a. Do different locomotor modes during growth modulate trabecular architecture in the murine hind limb? Integr Comp Biol 48:385–393.

Carlson K, Sumner D, Morbeck M, Nishida T, Yamanaka A, Boesch C. 2008b. Role of nonbehavioral factors in adjusting long bone diaphyseal structure in free-ranging *Pan troglodytes*. Int J Primatol 29:1401–1420.

Cotter M, Simpson S, Latimer B, Hernandez C. 2009. Trabecular microarchitecture of hominoid thoracic vertebrae. Anat Rec 292:1098–1106.

Cowin S. 1986. Wolff's law of trabecular architecture at remodeling equilibrium. J Biomed Eng 108:83–88.

Currey J. 1984. The mechanical adaptation of bones. Princeton: Princeton University Press.

Curtin S, Chivers D. 1978. Leaf-eating primates of peninsular Malaysia: the siamang and the dusky leaf monkey. In: Montgomery G, editor. The ecology of arboreal folivores. Washington, DC: Smithsonian Institution Press. p 441–464.

Demes B, Carlson K. 2009. Locomotor variation and bending regimes of Capichin limb bones. Am J Phys Anthropol 139:558–571.

Demes B, Carlson K, Franz T. 2006. Cutting corners: the dynamics of turning behaviors in two primate species. J Exp Biol 209:927–937.

Demes B, Franz T, Carlson K. 2005. External forces on the limbs of jumping lemurs at takeoff and landing. Am J Phys Anthropol 128:348–358.

Demes B, Larson J, Stern J, Jungers W, Biknevicus A, Schmitt D. 1994. The kinetics of primate quadrupedalism: "hindlimb drive" reconsidered. J Hum Evol 26:353–374.

Doran D. 1993. Sex differences in adult chimpanzee positional behavior: the influence of body size on locomotion and posture. Am J Phys Anthropol 91:99–115.

Doube M, Klowowski M, Wiktorowicz-Conroy A, Hutchinson J, Shefelbine S. 2011. Trabecular bone scales allometrically in mammals and birds. Proc R Soc Lond B Biol Sci. doi: 10.1098/rspb.2011.0069.

Fajardo R, Müller R. 2001. Three-dimensional analysis of nonhuman primate trabecular architecture using micro-computed tomography. Am J Phys Anthropol 115:327–336.

Fajardo R, Müller R, Ketcham R, Colbert M. 2007. Nonhuman anthropoid primate femoral neck trabecular architecture and its relationship to locomotor mode. Anat Rec 290:422–436.

Fleagle J. 1976. Locomotion and posture of the Malayan siamang and implications for hominoid evolution. Folia Primatol (Basel) 26:245–269.

Fleagle J. 1988. Primate evolution and adaptation. New York: Academic Press.
Goldstein S, Goulet R, McCubbrey D. 1993. Measurement of significance of three-dimensional architecture to the mechanical integrity of trabecular bone. Calcif Tissue Int 53:S127–S133.
Griffin N, D'Aout K, Ryan T, Richmond B, Ketcham R, Postnov A. 2010. Comparative forefoot trabecular bone architecture in extant hominids. J Hum Evol 59:202–213.
Haapasalo H, Kontulainen S, Sievanen H, Kannus P, Jarvinen M, Vuori I. 2000. Exercise-induced bone gain is due to enlargement in bone size without a change in volumetric bone density: a peripheral quantitative computed tomography study of the upper arms of male tennis players. Bone 27:351–357.
Hanna J, Polk J, Schmitt D. 2006. Forelimb and hindlimb forces in walking and galloping primates. Am J Phys Anthropol 130:529–535.
Harrigan T, Jasty M, Mann R, Harris W. 1988. Limitations of the continuum assumption in cancellous bone. J Biomech 21:269–275.
Harrigan T, Mann R. 1984. Characterization of microstructural anisotropy in orthotropic materials using a second rank tensor. J Mater Sci 19:761–767.
Heinonen A, Sievanen H, Kannus P, Oja O, Vuori I. 2002. Site-specific skeletal response to long-term weight training seems to be attributable to principal loading modality: a pQCT study of female weightlifters. Calcif Tissue Int 70:469–474.
Hildebrand T, Ruegsegger P. 1997a. A new method for the model-independent assessment of thickness in three-dimensional images. J Microsc 185:67–75.
Hildebrand T, Ruegsegger P. 1997b. Quantification of bone microarchitecture with structure model index. Comp Meth Biomech Biomed Eng 1:15–23.
Hirasaki E, Kumakura H, Matano S. 2000. Biomechanical analysis of vertical climbing in the spider monkey and the Japanese macaque. Am J Phys Anthropol 113:455–472.
Holt BM. 2003. Mobility in upper paleolithic and mesolithic Europe: evidence from the lower limb. Am J Phys Anthropol 122:200–215.
Jones HH, Priest JD, Hayes WC, Tichenor CC, Nagel DA. 1977. Humeral hypertrophy in response to exercise. J Bone Joint Surg Am 59A:204–208.
Kabel J, van Rietbergen B, Odgaard A, Huiskes R. 1999. Constitutive relationships of fabric, density, and elastic properties in cancellous bone architecture. Bone 25:481–486.
Ketcham R, Ryan T. 2004. Quantification and visualization of anisotropy in trabecular bone. J Microsc 213:158–171.
Kimura T. 1985. Bipedal and quadrupedal walking of primates: comparative dynamics. Primate morphophysiology, locomotor analyses and human bipedalism. Tokyo: University of Tokyo Press. p 81–104.
Kimura T. 1992. Hind limb dominance during primate high-speed locomotion. Primates 33:465–476.
Kummer B. 1972. Biomechanics of bone: mechanical properties, functional structure, functional adaptation. In: Fung Y, Perrone N, Anliker M, editors. Biomechanics: its foundations and objectives. Englewood Cliffs, NJ: Prentice-Hall Inc. p 237–271.
Lanyon LE. 1992. Control of bone architecture by functional load bearing. J Bone Miner Res 7:S369–S375.
Lazenby R, Angus S, Cooper D, Hallgrimsson B. 2008. A three-dimensional microcomputed tomographic study of site-specific variation in trabecular microarchitecture in the human second metacarpal. J Anat 213:698–705.
Macdonald H, Cooper D, McKay H. 2009. Anterior-posterior bending strength at the tibial shaft increases with physical activity in boys: evidence for non-uniform geometric adaptation. Osteoporos Int 20:61–70.
Macdonald H, Kontulainen S, MacKelvie-O'Brien K, Petit M, Janssen P, Khan K, McKay H. 2005. Maturity- and sex-related changes in tibial bone geometry, strength and bone-muscle strength indices during growth: A 20month pQCT study. Bone 36:1003–1011.
MacDougall J, Webber C, Martin J, Omerod S, Chesley A, Younglai E, Gordon C, Blimkie C. 1992. Relationship among running mileage, bone density, and serum testosterone in male runners. J Appl Physiol 73:1165–1170.
MacLatchy L, Müller R. 2002. A comparison of the femoral head and neck trabecular architecture of *Galago* and *Perodicticus* using micro-computed tomography (uCT). J Hum Evol 43:89–105.
Marchi D. 2005. The cross-sectional geometry of the hand and foot bones of the Homonoidea and its relationship to locomotor behavior. J Hum Evol 49:743–761.
Marchi D. 2007. Relative strength of the tibia and fibula and locomotor behavior in hominoids. J Hum Evol 53:647–655.
Marchi D. 2008. Relationships between lower limb cross-sectional geometry and mobility: the case of a Neolithic sample from Italy. Am J Phys Anthropol 137:188–200.
Martin B, Burr DR, Sharkley N. 1998. Skeletal tissue mechanics. New York: Springer-Verlag, Inc.
Napier J, Napier P. 1967. A handbook of living primates. London: Academic Press.
Neville M, Glander K, Braza F, Rylands A. 1988. The howling monkeys, genus *Alouatta*. In: Mittermeier R, Rylands AB, Coimbra-Filho A, de Fonseca G, editors. Ecology and behavior of Neotropical primates. Washington, DC: World Wildlife Fund. p 349–453.
Nikander R, Sievanen H, Uusi-Rasi K, Heinon A, Kannus P. 2006. Loading modalities and bone structure at nonweight-bearing upper extremity and weight-bearing lower extremity: a pQCT study of adult female athletes. Bone 39:886–894.
O'Neill M, Dobson S. 2008. The degree and pattern of phylogenetic signal in primate long-bone structure. J Hum Evol 54:309–322.
Odgaard A. 1997. Three-dimensional methods for the quantification of cancellous bone architecture. Bone 20:315–328.
Odgaard A, Gundersen H. 1993. Quantification of connectivity in cancellous bone, with special emphasis on 3D reconstruction. Bone 14:173–182.
Oxnard C, Yang H. 1981. Beyond biometrics: studies of complex biological patterns. Symp Zool Soc Lond 46:127–167.
Patel B, Carlson K. 2008. Apparent density patterns in subchondral bone of the sloth and anteater forelimb. Biol Lett 4:486–489.
Pauwels F. 1980a. Biomechanics of the locomotor apparatus: contributions on the functional anatomy of the locomotor apparatus. Berlin: Springer-Verlag.
Pauwels F. 1980b. Principles of construction of the lower extremity. Their significance for the stressing of the skeleton in the leg. In: Pauwels F, editor. Biomechanics of the locomotor aparatus. Berlin: Springer-Verlag. p 193–204.
Payseur B, Covert H, Vinyard C, and Dagosto M. 1999. New body mass estimates for *Omomys carteri*, a middle Eocene primate from North America. Am J Phys Anthropol 109:41–52.
Pearson OJ, Lieberman DE. 2004. The aging of Wolff's "law": ontogeny and responses to mechanical loading in cortical bone. Yrbk Phys Anthropol 47:63–99.
Pontzer H, Lieberman DE, Momin E, Devlin MJ, Polk JD, Hallgrimsson B, Cooper D. 2006. Trabecular bone in the bird knee responds with high sensitivity to changes in load orientation. J Exp Biol 209:57–65.
Radin E, Orr R, Kelman J, Paul I, Rose R. 1982. Effect of prolonged walking on concrete on the knees of sheep. J Biomech 15:487–492.
Rafferty K. 1998. Structural design of the femoral neck in primates. J Hum Evol 34:361–383.
Rafferty K, Ruff C. 1994. Articular structure and function in *Hylobates*, *Colobus*, and *Papio*. Am J Phys Anthropol 94:395–408.
Ridler TW, Calvard S. 1978. Picture thresholding using an iterative selection method. IEEE Trans Syst Man Cybern SMC 8:630–632.
Rodman P. 1977. Feeding behavior of Orangutans of the Kutai nature reserve, east Kalimantan. In: Clutton-Brock T, editor. Primate ecology: studies of feeding and ranging behaviour in lemurs, monkeys, and apes. London: Academic Press. p 384–414.
Rowe N. 1999. The pictorial guide to the living primates. Charlestown, RI: Pogonias Press.
Rubin C, Lanyon LE. 1984. Dynamic strain similarity in vertebrates; an alternative to allometric limb bone scaling. J Theor Biol 107:321–327.

Rubin C, Lanyon LE. 1985. Regulation of bone mass by mechanical strain magnitude. Calcif Tissue Int 37:411–417.
Rubin C, McLeod K, Basin S. 1990. Functional strains and cortical bone adaptation: epigenetic assurance of skeletal integrity. J Biomech 23 (Suppl 1):43–54.
Ruff C. 1987. Structural allometry of the femur and tibia in Hominoidea and *Macaca*. Folia Primatol (Basel) 48:9–49.
Ruff C, Scott W, Liu A. 1991. Articular and diaphyseal remodeling of the proximal femur with changes in body mass in adults. Am J Phys Anthropol 86:397–413.
Ruff C. 2002. Long bone articular and diaphyseal structure in Old World monkeys and apes. I. Locomotor effects. Am J Phys Anthropol 119:305–342.
Ruff CB. 2003. Long bone articular and diaphyseal structure in old world monkeys and apes. II: Estimation of body mass. Am J Phys Anthropol 120:16–37.
Ruff C. 2008. Femoral/humeral strength in early African *Homo erectus*. J Hum Evol 54:383–390.
Ruff C. 2009. Relative limb strength and locomotion in *Homo habilis*. Am J Phys Anthropol 138:90–100.
Ruff CB. 2000. Body size, body shape and long bone strength in modern humans. J Hum Evol 38:269–290.
Ruff CB, Holt BM, Trinkaus E. 2006. Who's afraid of the big bad Wolff? "Wolff's Law" and bone functional adaptation. Am J Phys Anthropol 129:484–498.
Ruff CB, Runestad J. 1992. Primate limb bone structural adaptations. Ann Rev Anthropol 21:407–433.
Ryan T, Colbert M, Ketcham R, Vinyard J. 2010. Trabecular bone structure in the mandibular condyles of gouging and nongouging Platyrrhine primates. Am J Phys Anthropol 141:583–593.
Ryan T, Ketcham R. 2002. The three-dimensional structure of trabecular bone in the femoral head os strepsirrhine primates. J Hum Evol 43:1–26.
Ryan T, Ketcham R. 2005. Angular orientation of trabecular bone in the femoral head and its relationship to hip joint loads in leaping primates. J Morphol 265:249–263.
Ryan T, van Rietbergen B. 2005. Mechanical significance of femoral head trabecular bone structure in *Loris* and *Galago* evaluated using micromechanical finite element models. Am J Phys Anthropol 126:82–96.
Ryan T, Walker A. 2010. Trabecular bone structure in the humeral and femoral heads of anthropoid primates. Anat Rec 293:719–729.
Sarringhaus L, Stock JT, Marchant L, McGrew W. 2005. Bilateral asymmetry in the limb bones of the chimpanzee (*Pan troglodytes*). Am J Phys Anthropol 127:840–845.
Schaffler M, Burr D, Jungers W, Ruff C. 1985. Structural and mechanical indicators of limb specialization in primates. Folia Primatol (Basel) 45:61–75.
Scherf H. 2008. Locomotion-related femoral trabecular architectures in primates—high resolution computed tomographies and their implications for estimations of locomotor preferences of fossil primates. In: Endo H, Frey R, editors. Anatomical imaging: towards a new morphology. Tokyo: Springer. p 38–59.
Schmitt D, Hanna J. 2004. Substrate alters forelimb to hindlimb peak force ratios in primates. J Hum Evol 46:149–159.
Shaw C, Stock J. 2009a. Habitual throwing and swimming correspond with upper limb diaphyseal strength and shape in modern human athletes. Am J Phys Anthropol 140:160–172.
Shaw C, Stock J. 2009b. Intensity, repetitiveness, and directionality of habitual adolescent mobility patterns influence the tibial diaphysis morphology of athletes. Am J Phys Anthropol 140:149–159.
Stock J. 2006. Hunter-gatherer postcranial robusticity relative to patterns of mobility, climatic adaptation, and selection for tissue economy. Am J Phys Anthropol 131:194–204.
Stock J, Pfeiffer S. 2001. Linking structural variability in long bone diaphyses to habitual behaviors: foragers from the southern African Later Stone Age and the Andaman Islands. Am J Phys Anthropol 115:337–348.
Swartz S. 1989. The functional morphology of weight bearing: limb joint surface area allometry in anthropoid primates. J Zool 218:441–460.
Swartz S, Bertram J, Biewener A. 1989. Telemetered *in vivo* strain analysis of locomotor mechanics of brachiating gibbons. Nature 342:270–272.
Trussell HJ. 1979. Comments on "Picture thresholding using an iterative selection method." IEEE Trans Syst Man Cybern SMC 9:311.
Ulrich D, van Rietbergen B, Laib A, Rüegsegger P. 1999. The ability of three-dimensional structural indices to reflect mechanical aspects of trabecular bone. Bone 25:55–60.
Vainionpaa A, Korpelainen R, Sievanen H, Vihriala E, Leppatuoto J, Jamsa T. 2007. Effect of impact exercise and its intensity on bone geometry at weight-bearing tibia and femur. Bone 40:604–611.
Ward S, Sussman R. 1979. Correlates between locomotor anatomy and behavior in two sympatric species of Lemur.50:575–590.
Whitehouse W. 1974. The quantitative morphology of anisotropic trabecular bone. J Microsc 101:153–168.